

Sensitivity Analysis and Uncertainty Quantification for Crystal Plasticity Parameters of Ti-6Al-4V Alloy

Mohamed Elleithy * and Pınar Acar[†] Virginia Tech, Blacksburg, VA-24061

This study presents a comprehensive investigation into the crystal plasticity behavior of the dual-phase Ti-6Al-4V alloy through the utilization of Crystal Plasticity Finite Element (CPFE) modeling and subsequent calibration. Employing a rate-independent, single-crystal constitutive model, the calibration process integrates an interior-point optimization algorithm with experimental data, yielding precise predictions for crystal plasticity (CP) parameters. Uncertainty quantification (UQ) through Monte Carlo Sampling (MCS) method reveals the impact of CP parameters and their uncertainty on the alloy's elasto-plastic mechanical properties. Sensitivity analysis further elucidates the influence of slip-system specific parameters on the alloy's elastic and plastic behavior, emphasizing the role of initial slip resistance as a critical determinant in both regimes. The research findings contribute to a deeper understanding of CP modeling of Ti-6Al-4V alloy and its implications for materials design.

Nomenclature

 $\delta^{\alpha\beta}$ = Kronecker delta function

 σ_{yield} = Yield strength

a = Power law exponent

 $b_{i=1,...,4}$ = Plastic-region characteristic slopes C_{ij} = Constitutive elastic stiffness tensor

E = Elastic modulus $h^{\alpha\beta}$ = Hardening moduli

 h^{β} = Single-crystal hardening modulus

 h_0 = Initial hardening modulus q = Latent hardening ratio s^{β} = Critical resolved shear stress

 s_s = Saturation stress s_0 = Initial slip resistance SSE = Sum of Squared Error

I. Introduction

Recent advancements in structural and materials engineering have focused on the optimization of Titanium alloy microstructures for a finer mechanical performance. The crystal plasticity finite element method (CPFEM) has shown promise in accurately predicting the micro-mechanical behavior of Ti-6Al-4V components, incorporating micro-scale defect analysis to enhance the efficacy of industrial applications [1]. The significance of microstructural analysis is underscored by studies that utilize CPFEM to correlate these characteristics with the mechanical properties of Titanium alloys [2]. Innovations in Titanium alloy composition and casting techniques, informed by numerical strategies developed upon the introduction of the Integrated Computational Materials Engineering (ICME) paradigm, are set to reduce manufacturing costs while maintaining the material's functional integrity [3–5]. Additionally, the integration of CPFEM and machine learning (ML) within the Parametrically Homogenized Constitutive Model (PHCM) framework provides a robust tool for simulating the mechanical behavior of dual-phase Titanium alloys [6]. Lastly, the critical role of the beta-phase in the high-cycle fatigue behavior of Ti-6Al-4V alloys has been highlighted through

^{*}Graduate Research Assistant, MS.c. Student, Department of Mechanical Engineering, AIAA Student Member

[†]Assistant Professor, Department of Mechanical Engineering, AIAA Member

ultrasonic fatigue testing and CPFEM simulations, thus motivating the explicit phase-definition in CPFEM simulations as portrayed in the scope of this research [7].

Ti-6Al-4V, known as Grade 5 Titanium, is a predominant alpha-beta Titanium alloy extensively utilized in the aerospace industry for its exceptional combination of durability, lightweight, and resistance to corrosion [8]. The alloy incorporates Aluminum to stabilize the alpha-phase and Vanadium to stabilize the beta-phase, resulting in a robust microstructure that combines both equiaxed alpha patterns and beta regions [9]. This microstructure is especially advantageous for aerospace components, which require corrosion-resistant materials that can withstand high stress while minimizing weight to enhance performance. In the aerospace sector, Ti-6Al-4V is used in the manufacturing of critical engine components, airframes, and landing gears [10]. The unique properties of the alloy allow it to perform under the high temperatures and dynamic stresses encountered during flight [11]. Overall, the importance of Ti-6Al-4V in aerospace cannot be overstated, with its combination of exceptional mechanical properties, adaptability to advanced manufacturing processes, and potential for improved performance ensuring its continued use and development within the industry [10, 12].

Uncertainty quantification (UQ) is essential for the validation of computational models in materials science, such as those predicting material behavior through CPFEM. UQ ensures confidence in a model's predictive capabilities by accounting for potential variability and unknowns within the modeling process. Recent advances in ICME leverage CPFEM to bridge the gap between microstructural behavior and material properties [13–16]. These models bypass the need for extensive experimentation, streamlining the material design process under initiatives like the Material Genome Initiative [17]. The reliability of CPFEM, however, hinges on the constitutive models' precision. Studies have shown considerable variability in CPFEM predictions when parameters change, indicating the need for robust sensitivity analysis and UQ [18]. To enhance the accuracy of novel CPFE methods for materials like alpha-beta Titanium alloys, the evaluation of slip dislocation criteria within the constitutive models is imperative. Different numerical methods incorporate image processing, modeling of dislocation slip transfer, and Bayesian calibration, ultimately leading to the development of CPFEM strategies to investigate the mechanical behavior of complex microstructures [19].

Furthermore, the inherent uncertainty in calibrating CPFEM parameters is addressed through a genetic algorithm, defining the distribution of parameters and their effect on model predictions, such as stress and plastic strain [20]. This provides a framework for quantifying the variability due to parameter uncertainty, which is crucial for the model's predictive accuracy. Recent efforts to integrate UQ into CPFEM underscore the critical role UQ plays in both the verification and validation of ICME and ML models, aiming to understand homogenized properties within a broader context [21, 22].

Sensitivity analysis of crystal plasticity (CP) parameters has also been a focus of research aimed at enhancing the understanding of micro-mechanical behavior. Studies have shown that accurately matching the deformation of real polycrystals with predictions from CP models requires precise representation of 3D microstructures and boundary conditions [23, 24]. However, the influence of material parameters on local polycrystal responses has not been extensively explored for the constitutive plasticity model operated. Through the application of UQ and sensitivity analysis on polycrystalline microstructure models using CP, researchers have unveiled significant variations in stress and strain predictions stemming from changes in material parameters [23, 24]. Notably, sensitivity analysis has highlighted the high sensitivity of CP model solutions to parameters like latent hardening and the crystal orientations of grains, factors contributing significantly to the variability in model predictions [23, 24]. These insights are invaluable for refining CP models and advancing the ability to predict material behavior accurately [23, 24].

This study aims to achieve two main objectives. Firstly, it seeks to precisely calibrate CP parameters for the Ti-6Al-4V alloy by utilizing a CPFE model and interior-point optimization as outlined by the closed-loop schematic in Figure 1. Secondly, it aims to assess the impact of parameter uncertainties and sensitivities on the alloy's elastic and plastic behavior. In Section II, "Computational Modeling", the methodology is outlined. This section elaborates on the CPFE modeling approach, emphasizing the integration of a rate-independent, single-crystal constitutive model. The utilization of an interior-point optimization algorithm for calibration is also discussed to ensure precise parameter approximation relative to the compressive experimentation results provided. Section III, "Results and Discussion", underlines the research findings through 3 main categories: (1) Calibration Results for Crystal Plasticity Parameters, presenting candid parameters for the Ti-6Al-4V alloy at ambient temperature; (2) Uncertainty Quantification Results for Crystal Plasticity Parameters, revealing the influence of parameter variations on mechanical properties; and (3) Sensitivity Analysis Results for Crystal Plasticity Parameters, highlighting the significance of slip-system specific parameters in the alloy's elastic and plastic behavior. Section IV, "Conclusion", provides a concise summary of the study's key findings, underlining the importance of accurate parameter estimation in CP modeling.

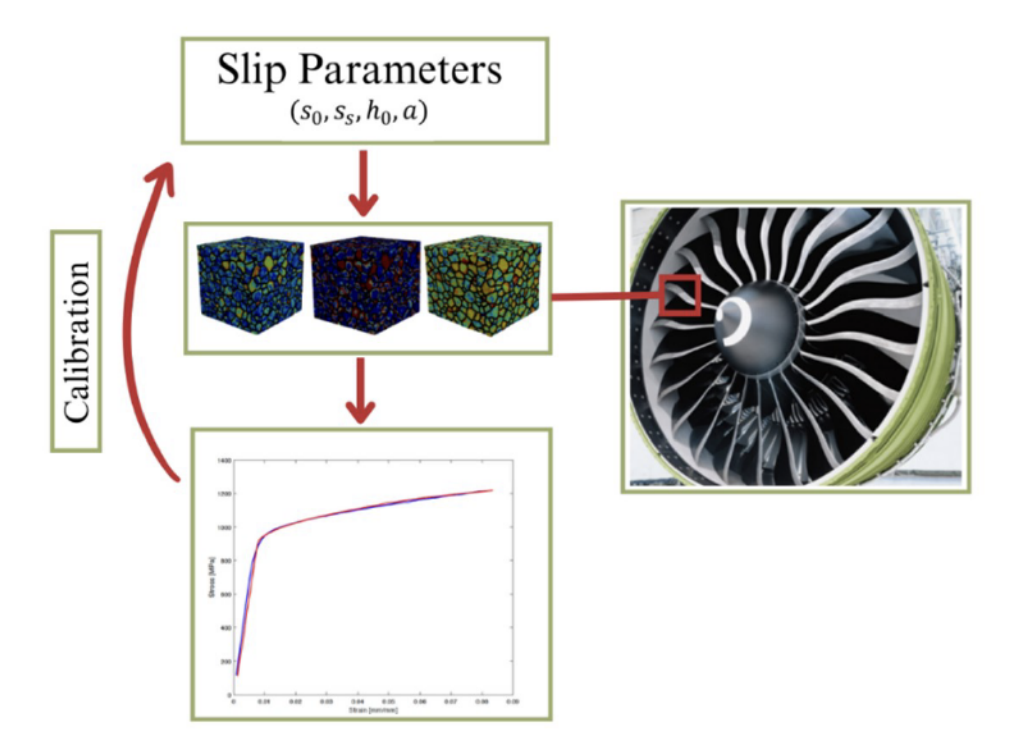


Fig. 1 The proposed multi-scale schematic to study mechanical properties with the calibration of the CP model (Image of GE90 Engine - Courtesy of General Electric) [25]

II. Computational Framework

A. Crystal Plasticity Finite Element (CPFE) Modeling

The incorporation of a Crystal Plasticity Finite Element (CPFE) model provides a precise multi-scale framework, enabling the examination of both elastic and plastic mechanical properties of the dual-phase Ti-6Al-4V alloy. A proprietary CPFE model considers the microscopic texture with granular orientations, phase-specific dislocation slip-systems, and single-crystalline values for the elasticity constitutive tensor (C_{ij}), along with the slip hardening parameters. This approach aims to predict the elasto-plastic mechanical behavior of Ti-6Al-4V under predefined boundary conditions efficiently. For this investigation, the rate-independent, single-crystal plasticity constitutive model developed by Anand and Kothari [26] is chosen. This choice facilitates the calibration of the Ti-6Al-4V CP parameters at 21^{o} C, further enabling the prediction of the dual-phase alloy's homogenized (volume-averaged) stress-strain behavior. The hardening moduli ($h^{\alpha\beta}$), fundamental to the aforementioned model, conforms to the equation as delineated in Refs. [26–28]:

$$h^{\alpha\beta} = [q + (1 - q)\delta^{\alpha\beta}]h^{\beta} \quad \text{(no sum on } \beta)$$
 (1)

In this equation, $\delta_{\alpha\beta}$ symbolizes the Kronecker delta function, while q signifies the latent hardening ratio, and h_{β} denotes the single-crystal slip hardening rate. Generally, the values 1.0 and 1.4 serve to define the latent hardening ratio in alignment with a coplanar and non-coplanar slip system, respectively. It is assumed that the slip systems of the Hexagonal Close-Packed (HCP) microstructure are non-coplanar [29]. Conversely, simulations of the Body-Centered Cubic (BCC) microstructure presume a coplanar slip system [29]. An inclusive expression for the single-crystal slip hardening rate, factoring in the alloy's hardening parameters h_0 , s_s , and a, is defined by Refs. [26–28]:

$$h^{\beta} = h_0 (1 - \frac{s^{\beta}}{s_s})^a \tag{2}$$

Within this context, h_0 represents the hardening modulus, s_s characterizes the saturation stress, s_β is defined as the critical resolved shear stress, and a embodies the power law exponent. The basal < a >, prismatic < a >, pyramidal < a >, and pyramidal first < c + a > slip systems are the primary considerations in this calibration study. Concerning the formulation of the elastic stiffness tensor for the HCP crystalline structure, prior to CPFE deformation simulation, it is posited on a transversely isotropic condition, adhering to the independence of five primary constituents. These conditions are stipulated as: $C_{11} = C_{22}$, C_{12} , $C_{13} = C_{23}$, C_{33} , C_{55} , and $C_{44} = (C_{11}-C_{12})/2$, as exhibited by data presented in Table 1. Concurrently, Table 2 elucidates beta-phase elastic stiffness in three independent components corresponding to a BCC structure. The stipulated conditions here are $C_{11} = C_{22} = C_{33}$, $C_{12} = C_{13} = C_{23}$, and $C_{44} = C_{55} = C_{66}$. The phase-specific elastic stiffness tensor values for both alpha and beta phases, calibrated near room temperature, find their basis in Refs. [30–32].

Table 1 Elastic constitutive tensor components for alpha-phase at 21°C [30–32]

C ₁₁	C ₃₃	C ₅₅	C_{12}	C ₁₃
164.7 GPa	82.5 GPa	61.8 GPa	175.2 GPa	48.5 GPa

Table 2 Elastic constitutive tensor components for beta-phase at 21°C [30–32]

C ₁₁	C ₅₅	C ₁₂
104.6 GPa	148.9 GPa	71.3 GPa

B. Calibration of CPFE Model Parameters via Optimization

The calibration of the hardening parameters of Ti-6Al-4V alloy at 21°C involves the integration of the CPFE model with an interior-point convex optimization method. Given the absence of analytical or experimental quantifications for the hardening parameters in the chosen constitutive model under a particular loading condition, the calibration process becomes imperative. The interior-point optimization method was selected for its efficiency in addressing large-scale optimization problems that encompass multiple active variables, and for its ability to learn from discretized data points to obtain a solution. The efficacy of the algorithm lies in its capability to assign a median between upper and lower bounds through the robust convergence of the objective function, thereby ensuring minimal computational time and pronounced numerical stability in tandem with a high-fidelity CPFE model.

In order to determine the optimal values for initial slip resistances (s_0) , hardening moduli (h_0) , saturation stress (s_s) , and power law exponent (a) within ambient room temperature conditions, stress-strain data acquired from experimental compression tests are incorporated into the optimization algorithm. The objective function is constructed to minimize the total of the squared relative error values between the predictions of the CPFE simulations and the corresponding experimental measurements. Formulating the sum of squared errors (SSE) as an objective function proves crucial to address the disparity in magnitude between the parameters of the stress-strain curve used in objective function generation. The optimization problem is depicted by the equation:

minimize
$$SSE(s_0, h_0, s_s, a)$$
 (3)

$$SSE = \left(\frac{E^{pred} - E^{exp}}{E^{exp}}\right)^2 + \left(\frac{\sigma_y^{pred} - \sigma_y^{exp}}{\sigma_y^{exp}}\right)^2 + \sum_{i=1}^4 \left(\frac{b_i^{pred} - b_i^{exp}}{b_i^{exp}}\right)^2$$
(4)

In the equation above, the terms pertain to the elastic modulus (E), yield strength (σ_y) , and four consecutive slope increments (b_i) where i=1,2,3,4 computed in the plastic deformation region of the stress-strain curve. The superscripts "exp" and "pred" signify experimental and predicted values, respectively. These parameters are delineated in Figure 2. The algorithm aims to derive a set of 10 independent design variables related to the CP hardening parameters at 21^o C. The values for initial slip resistance and the hardening moduli are tailored for basal (a), prismatic (a), pyramidal (a), and pyramidal (a), and pyramidal (a), and pyramidal (a), slip systems. In contrast, the saturation stresses and power law exponent are tailored to signify a singular variable for the HCP-specific slip-systems. Beta-phase hardening parameters are not categorized as separate variables in the calibration process due to the absence of definitive boundaries for the BCC slip

systems and the relatively small volume fraction of the beta phase (about 3%). Thus, these values are assumed to align with those of the alpha-phase basal < a >, prismatic < a >, and pyramidal < c + a >, grounded on the extrapolation of Ozturk et al.'s hypothesis in Refs. [32].

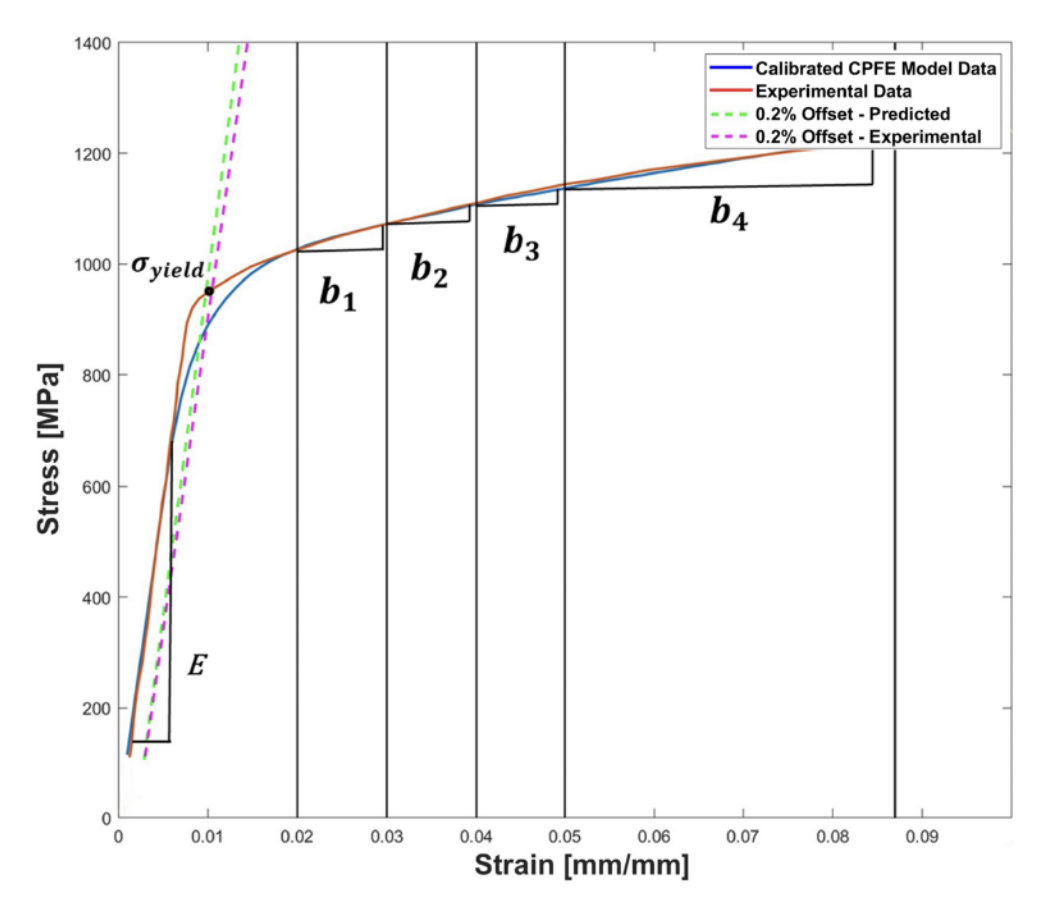


Fig. 2 Experimental and CPFE-predicted stress-strain curves for Ti-6Al-4V at room temperature

C. Uncertainty Quantification for Crystal Plasticity Parameters

Upon the completion of the CP parameters calibration at the benchmark temperature of 21^{o} C, a methodical uncertainty quantification (UQ) process is investigated. This process aims to assess the variability of homogenized elasto-plastic properties in response to perturbations of the CP parameters determined through optimization. To achieve this objective, the Monte Carlo Sampling (MCS) method is employed, capitalizing on its efficacy in handling large datasets and delivering reliable statistical outputs. The MCS approach uses a collection of 1000 samples of independent CP parameters, each subjecting the Ti-6Al-4V alloy to a 21^{o} C environment and a strain rate of $0.01 \text{ s}^{-}1$. Every sample incorporated random perturbations in the constitutive model's CP parameters, represented by a Gaussian distribution with a deviation of $\pm 10\%$ from their nominal values. Such simulations offer insights into the impact of microstructural parameters on homogenized elastic and plastic properties. The ability to trace variations in these properties to specific texture orientations becomes essential in ensuring that design and objective criteria align sufficiently within given constraints.

D. Sensitivity Analysis of Crystal Plasticity Parameters

The sensitivity assessment of the calibrated CP model is conducted on Ti-6Al-4V alloy. For this purpose, 10 independent CP parameters are explored within the scope of the study. In the sensitivity analysis, each slip-system [basal, prismatic, pyramidal, pyramidal first] was assigned unique values for s_0 and h_0 . This assignment was a direct result of how the optimization problem was structured, ensuring that the variations in s_0 and h_0 corresponded appropriately to each specific slip-system. Variations in parameters, s_s and a, are allocated to individual slip-systems for each sample.

Utilizing the MCS method, 20 samples are generated for each parameter within each slip-system under consideration for perturbation. Each variable is assumed to demonstrate a 10% perturbation, adhering to a uniform distribution. This methodology ensured an equal likelihood of occurrence for each variable's perturbation values. The primary objective is to evaluate the ramifications on the alloy's elastic and plastic behavior, with particular attention on the relative error values between the stress-strain curve parameters and the benchmark mechanical characteristics. Adopting a uniform distribution for parameter variation is motivated by the presently undefined relationship between the homogenized curve dependent variables and the CP model parameters. Limited literature exists detailing experimental investigations of these model parameters and their relation to the defined curve defining terms. This analysis aims to quantify the relative absolute error values between the specified elastic and plastic behavior parameters and discern the influence of particular CP parameters and their associated slip-systems on the mechanical attributes of Ti-6Al-4V.

III. Results and Discussion

A. Calibration Results for Crystal Plasticity Parameters

Leveraging the synergy between the CPFE model and the interior-point optimization algorithm yields specific CP parameters, as outlined in Table 1. For the Ti-6Al-4V microstructure, these values denote the optimum solution, constrained within the fixed upper and lower bounds of each active variable in the optimization framework. In alignment with the elastic and plastic descriptors in Figure 2, the model discerns a minimum of the objective function, while conforming to the pre-established bounds for the CP variables leveraging the research lab's preliminary work [28]. The stress-strain curve predicted by CPFE modeling in Figure 3 is juxtaposed with the experimental curve used in the calibration process. Any deviation observed in Figure 3 might originate from the inherent computational, epistemic errors of the CPFE model, specifically when interpolating sequential stress values during the simulation process to match with the corresponding experimental data. Augmenting the model with curve-fitting parameters, particularly during the transition from elastic to plastic deformation behavior, and refining the simulation's time-step could ameliorate this deviation. Nonetheless, it is imperative to acknowledge the potential computational overhead costs that the refinements may introduce. The rigorous calibration process, conducted under the stipulated temperature and strain rate, constructs a robust foundation for extrapolating the alloy's hardening trajectory. The calibration fortifies the predictive reliability of the model, rendering potential cost efficiencies in material experimentation processes. The optimal parameters, specific to Ti-6Al-4V, can be instrumental in advancing design strategies for analogous metallic alloys. Employing sophisticated design modalities like Computer-Aided Design (CAD) and Finite Element Method (FEM), particularly those capable of simulating avant-garde additive manufacturing paradigms, can optimize the creation of architectural components derived from Ti-6Al-4V. The calibration also lays the groundwork for a computational structure capable of adeptly accommodating variations in both ambient temperature and applied strain rate [29].

Table 3 Ti-6Al-4V (alpha-phase) calibrated crystal plasticity parameters at 21°C and strain-rate of 0.01 s⁻¹

Slip System	<i>s</i> ₀	h_0	Ss	a
Basal < a >	388.3 MPa	641.6 MPa	724.1 MPa	1.8
Prismatic < a >	383.7 MPa	509.9 MPa	724.1 MPa	1.8
Pyramidal < a >	686.3 MPa	610.2 MPa	724.1 MPa	1.8
Pyramidal $< c + a >$	423.8 MPa	642.1 MPa	724.1 MPa	1.8

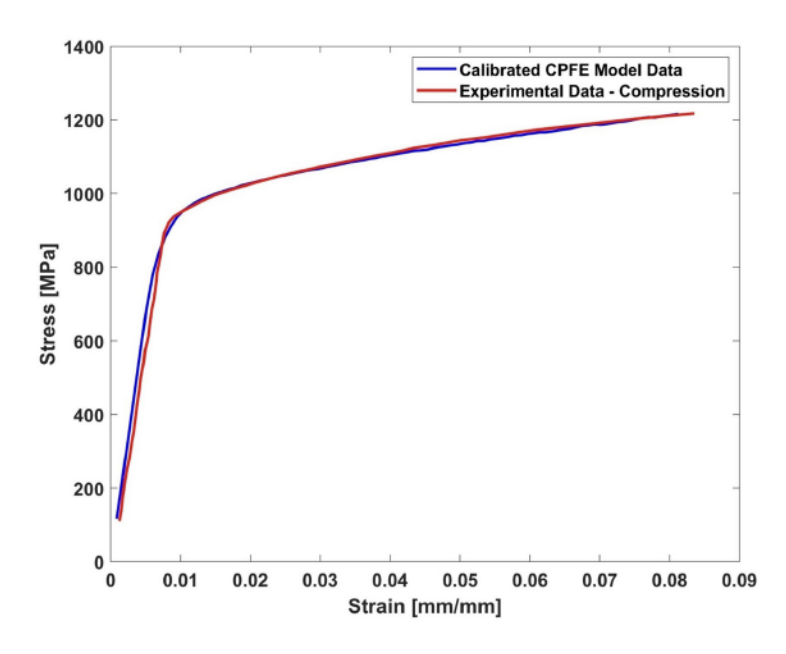


Fig. 3 Experimental data and calibrated CPFE prediction for Ti-6Al-4V stress-strain behavior

B. Uncertainty Quantification Results for Crystal Plasticity Parameters

Post calibration of the Ti-6Al-4V alloy-specific CP parameters, a Gaussian distribution spanning a $\pm 10\%$ range is defined to represent the uncertainty. This representation, derived from 1000 samples using the MCS method around the nominal/calibrated values of the CP parameters, is utilized to evaluate the model's responsiveness to the variations of CP parameters.

Figure 4 underscores the ramifications of a 10% variation of CP parameters on the alloy's mechanical behavior. The impact of this alteration is further corroborated by the Gaussian distribution patterns evident in the histogram plots for Young's modulus, yield strength, and plastic-region slopes, as portrayed in Figure 5 and Figure 6, respectively.

This 10% variation is primarily assumed; however, it is imperative to acknowledge potential contributors to the variability induced within the CP hardening parameters. Variables such as temperature fluctuations around a designated value, or strain rate deviations, can directly impinge on the CP parameters [32]. This introduces additional layers of uncertainty during the propagation of parameters in the CPFE simulation. Furthermore, the epistemic uncertainty intrinsic to the curve fitting of the stress-strain profile for obtaining the optimal set of calibrated parameters compounds this uncertainty. The quantitative analysis reveals the key parameters' ranges [minimum% – maximum%]) of error percentages evaluated in comparison between the nominal stress-strain curve and the set of 1000 generated stress-strain samples are as follows: Elastic Modulus [1.2e-3% - 8.4%], Yield Strength [1.1e-3% - 7.2%], b_1 [1.0e-3% - 12.3%], b_2 [4.3e-3% - 14.5%], b_3 [0.2% - 30.7%], and b_4 [3.4e-3% - 13.7%]. The lower percentages indicate the minimum error resultant from the perturbation within the calibrated CP parameters while the maximum error values demonstrate the largest variations observable in these properties. These values provide essential data on potential material design limits considering the specified 10% uncertainty in the system.

In summary, the findings demonstrate the extent to which a 10% change in the CP parameters influences the homogenized elastic and plastic properties. This underscores the critical nature of dependencies within the CP model, emphasizing the necessity for a detailed examination of uncertainties from an epistemic perspective.

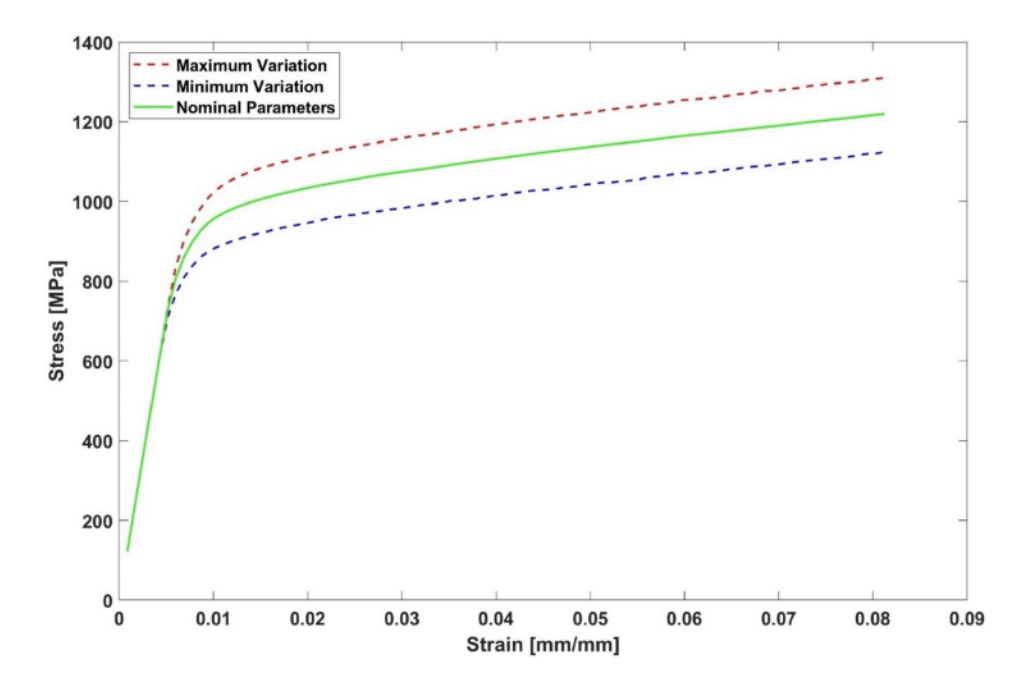


Fig. 4 Maximum and minimum stress-strain variations in response to 10% perturbation within CP parameters

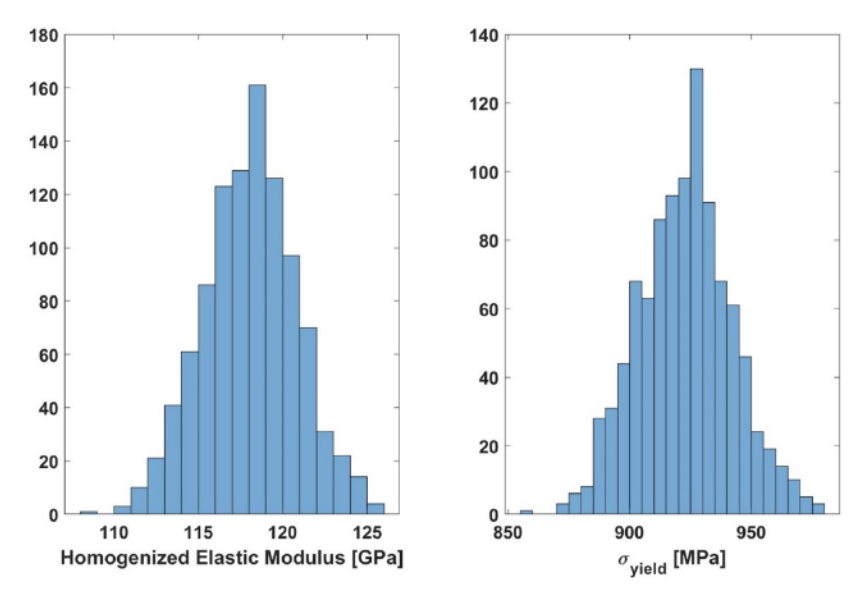


Fig. 5 $\,$ Frequency histograms for elastic modulus and yield strength in response to a 10% variation of optimal CP parameters

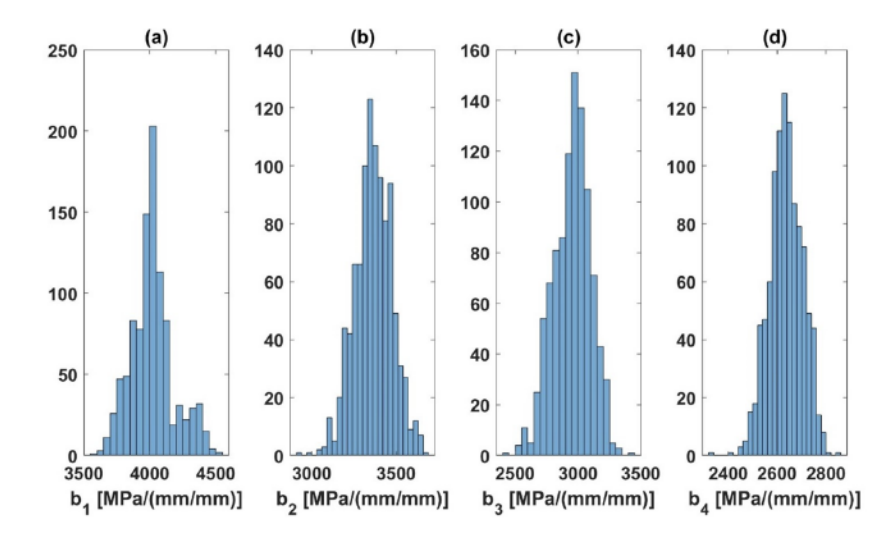


Fig. 6 Frequency histograms for plastic-region parameters in response to a 10% variation of optimal CP parameters

C. Sensitivity Analysis Results for Crystal Plasticity Parameters

Upon the computational evaluation of the elastic modulus and yield strength sensitivities at ambient temperature of 21^{o} C and a strain rate of 0.01 s^{-1} , the parameter s_0 is identified as the most critical determinant affecting the elastic properties of the material. As delineated in Figure 7, alterations in s_0 induce pronounced errors in the elastic modulus, culminating at a maximum error percentage of 4.74% for the pyramidal < a > slip-system, thereby indicating a substantial sensitivity of the alloy's elastic response to the initial slip resistance parameter. This pronounced deviation is mirrored in the yield strength, with an error margin of 3.74% as substantiated by Figure 8. In contrast, the perturbations applied to h_0 , s_s , and a do not precipitate significant fluctuations in the alloy's elastic performance, suggesting a relative insensitivity to these parameters under the tested conditions as illustrated by Figure 7-b and Figure 8-b. The data thus reveal a distinct hierarchy in parameter sensitivity, with s_0 potentially influencing the mechanical behavior of the alloy in the elastic regime, particularly within the pyramidal < a > slip-system.

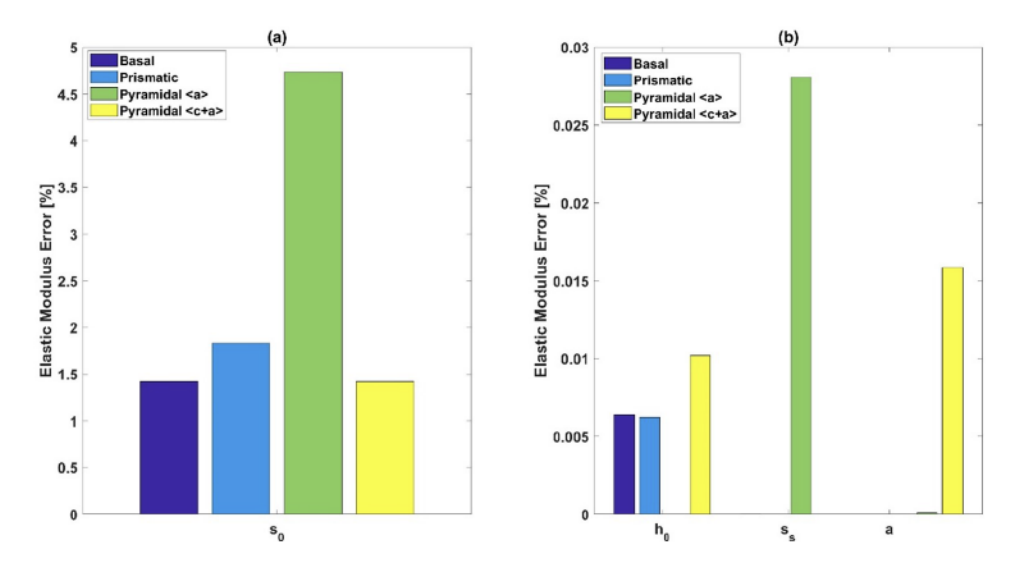


Fig. 7 Maximum error percentage for elastic modulus in response to 10% perturbation of each CP parameter

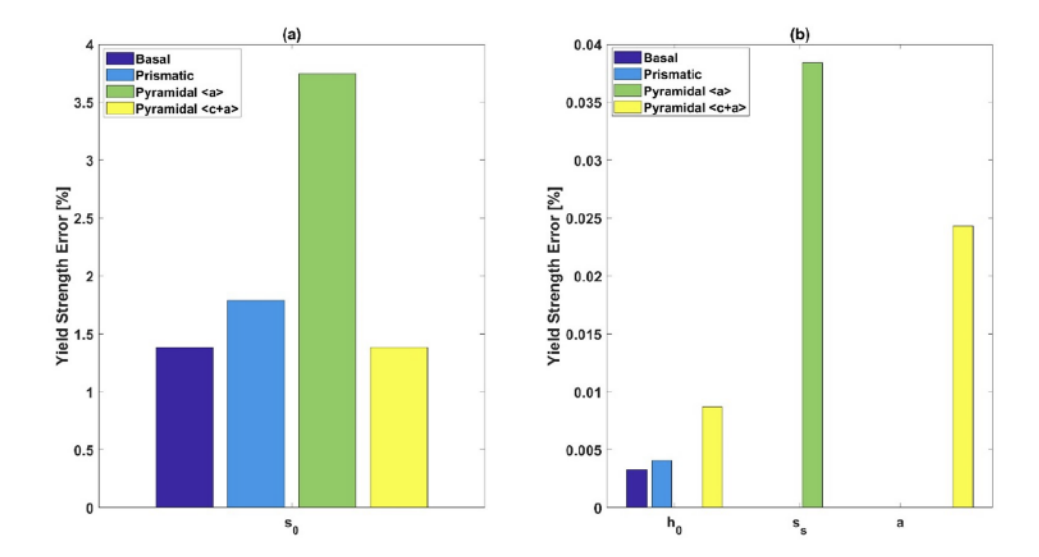


Fig. 8 Maximum error percentage for yield strength in response to 10% perturbation of each CP parameter

The analysis of b_i slopes in the plastic region of the dual-phase alloy confirms that CP parameters play a collective role in the prediction of plastic behavior. The predominance of s_0 as the critical factor influencing plastic performance is evident from the sensitivity values presented in Figure 9. Variations in the sensitivity of s_0 across different slip-systems, as shown in Figures 9 (a-d), suggest that each system may affect portions of the plastic region under compression, potentially in both simultaneous and sequential manners. s_0 , representing the necessary shear stress to initiate slip in each system, is reflected in Figure 9 (a-d) to correlate with the staged deformation sensitivity, consistent with the values in Table 3. The pyramidal < a > system demonstrates the highest resistance to deformation, indicating a greater s_0 is required to overcome this threshold. The response of both elastic and plastic parameters to a 10% perturbation of each CP parameter validates the optimization problem framework used in this study. The unchanged values of saturation stress (s_s) and power-law exponent (a) across different slip-systems, maintained during calibration, highlight the well-posed nature of the optimization problem. This is because the optimization problem defines more sensitive CP parameters as independent design variables for each slip system as established for the s_0 and s_0 parameters. In addition, less sensitive CP parameters are assumed to be dependent variables having the same value with the most dominant value across different slip systems to balance accuracy, computing times, and computational complexity.

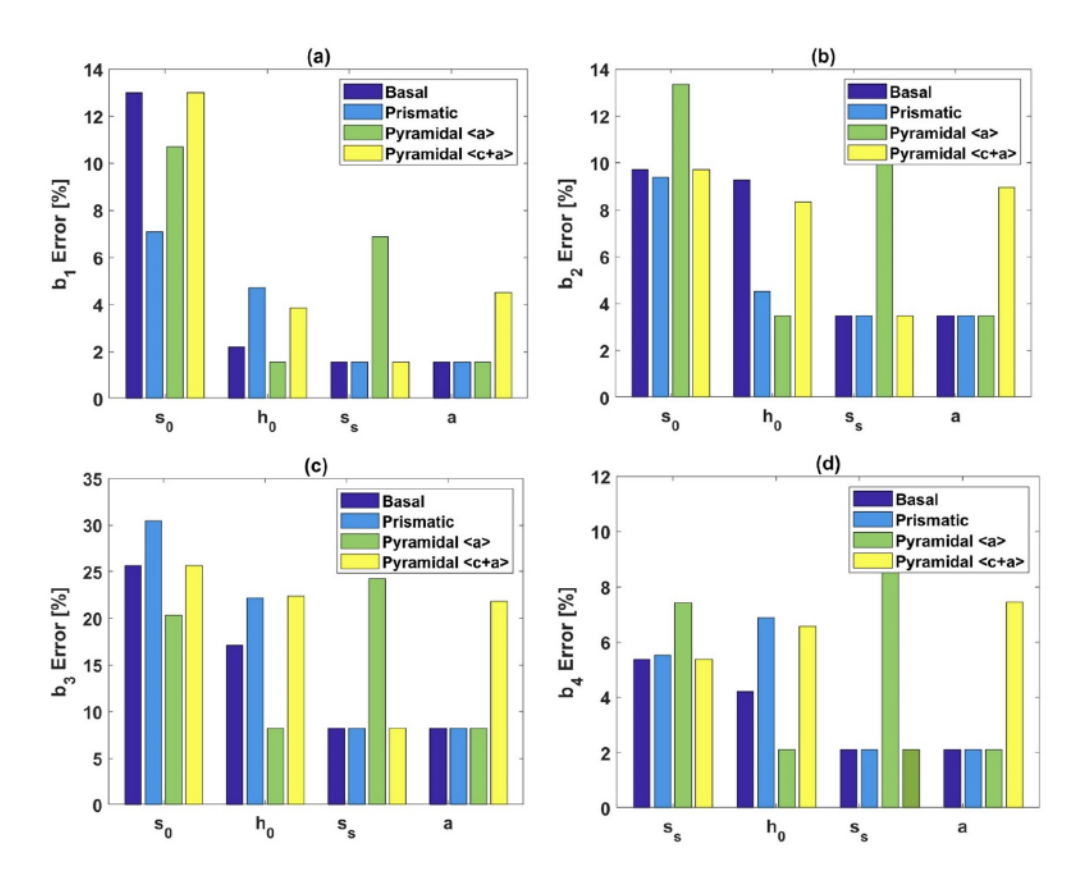


Fig. 9 Maximum error percentage for plastic region descriptors in response to 10% perturbation of each CP parameter

IV. Conclusion

In conclusion, the study has provided a rigorous exploration of Ti-6Al-4V alloy's mechanical behavior. The calibration process, facilitated by CPFE modeling and interior-point optimization, has enabled the determination of accurate CP parameters, bolstering the predictive reliability of the model. UQ results have revealed the potential implications of the parameters' perturbation, emphasizing the necessity for their precise determination. Sensitivity analysis has underscored the pivotal role of the initial slip resistance parameter in influencing both the elastic and plastic mechanical behavior of the alloy. The findings collectively enhance the understanding of the Ti-6Al-4V alloy's CP parameters and their correlation to the alloy's homogenized stress-strain characterization and offer valuable insights for materials design and simulation.

Looking forward, it is essential to recognize that there are other factors that may influence the behavior of metallic alloys such as Ti-6Al-4V on various hierarchies of scale. Understanding the physical phenomena's influence on the microstructure contributes to the comprehension of material deformation on a larger scale. Therefore, future investigations will focus on exploring factors such as temperature and strain rate on Ti-6Al-4V, as this would be essential in the development of surrogate models that may predict the alloy's thermo-mechanical performance at elevated temperatures while annihilating experimentation costs.

Acknowledgments

The authors acknowledge financial support from the NSF CMMI Award No. 2053840 (PD: Dr. Kathryn Jablokow) and the Young Faculty Award program by the Institute for Critical Technology and Applied Science (ICTAS) at Virginia Tech. We also thank Prof. John Allison from the Materials Science and Engineering Department at the University of Michigan and the Commonwealth Center for Advanced Manufacturing (CCAM) for the experimental data of Ti-Al alloys.

References

- Pinz, M., Storck, S., Montalbano, T., Croom, B., Salahudin, N., Trexler, M., and Ghosh, S., "Efficient computational framework for image-based micromechanical analysis of additively manufactured Ti-6Al-4V alloy," <u>Additive Manufacturing</u>, Vol. 60, 2022, p. 103269.
- [2] Thomas, J., Groeber, M., and Ghosh, S., "Image-based crystal plasticity FE framework for microstructure dependent properties of Ti-6Al-4V alloys," Materials Science and Engineering: A, Vol. 553, 2012, pp. 164-175.
- [3] Chang, X. Y., Shen, Q., Fan, W. X., and Hao, H., "Optimization of magnesium alloy casting process: an integrated computational materials engineering (icme) approach," Materials Science Forum, Vol. 1035, Trans Tech Publ, 2021, pp. 808–812.
- [4] Allison, J., Backman, D., and Christodoulou, L., "Integrated computational materials engineering: a new paradigm for the global materials profession," Jom, Vol. 58, 2006, pp. 25–27.
- [5] Cotton, J., Frohlich, C., and Glamm, R., "What boeing wants from integrated computational materials engineering for metallic materials," <u>53rd AIAA/ASME/ASCE/AHS/ASC Structures</u>, <u>Structural Dynamics and Materials Conference 20th</u> AIAA/ASME/AHS Adaptive Structures Conference 14th AIAA, 2012, p. 1407.
- [6] Kotha, S., Ozturk, D., and Ghosh, S., "Uncertainty-quantified parametrically homogenized constitutive models (UQ-PHCMs) for dual-phase α/β titanium alloys," NPJ Computational Materials, Vol. 6, No. 1, 2020, p. 117.
- [7] Chen, C., Gao, T., Chen, T., Li, B., Qin, Z., Chen, R., and Xue, H., "Experimental investigation and crystal plasticity simulation for the fatigue crack initiation of the equiaxed Ti-6Al-4V alloy in the very high cycle regime," <u>Engineering Failure Analysis</u>, 2023, p. 107427.
- [8] Khorasani, A. M., Goldberg, M., Doeven, E. H., and Littlefair, G., "Titanium in biomedical applications—properties and fabrication: a review," Journal of biomaterials and tissue engineering, Vol. 5, No. 8, 2015, pp. 593–619.
- [9] Seshacharyulu, T., Medeiros, S., Frazier, W., and Prasad, Y., "Hot working of commercial Ti–6Al–4V with an equiaxed α–β microstructure: materials modeling considerations," <u>Materials Science and Engineering: A</u>, Vol. 284, No. 1-2, 2000, pp. 184–194.
- [10] Veiga, C., Davim, J. P., and Loureiro, A., "Properties and applications of titanium alloys: a brief review," Rev. Adv. Mater. Sci. Vol. 32, No. 2, 2012, pp. 133–148.
- [11] Samuel, M. P., Mishra, A. K., and Mishra, R., "Additive manufacturing of Ti-6Al-4V aero engine parts: qualification for reliability," Journal of Failure Analysis and Prevention, Vol. 18, No. 1, 2018, pp. 136–144.
- [12] Yurtkuran, H., "An evaluation on machinability characteristics of titanium and nickel based superalloys used in aerospace industry," İmalat Teknolojileri ve Uygulamaları, Vol. 2, No. 2, 2021, pp. 10–29.
- [13] Aagesen, L., Adams, J., Allison, J., Andrews, W., Araullo-Peters, V., Berman, T., Chen, Z., Daly, S., Das, S., DeWitt, S., et al., "Prisms: An integrated, open-source framework for accelerating predictive structural materials science," <u>JOM</u>, Vol. 70, 2018, pp. 2298–2314.
- [14] Stopka, K. S., Yaghoobi, M., Allison, J. E., and McDowell, D. L., "Simulated effects of sample size and grain neighborhood on the modeling of extreme value fatigue response," Acta Materialia, Vol. 224, 2022, p. 117524.
- [15] Veasna, K., Feng, Z., Zhang, Q., and Knezevic, M., "Machine learning-based multi-objective optimization for efficient identification of crystal plasticity model parameters," <u>Computer Methods in Applied Mechanics and Engineering</u>, Vol. 403, 2023, p. 115740.
- [16] Wang, X., Liu, Y., Song, Y., Li, H., Hu, X., and Ji, Y., "Application of neural network in micromechanical deformation behaviors of Inconel 740H alloy," <u>The International Journal of Advanced Manufacturing Technology</u>, Vol. 125, No. 5-6, 2023, pp. 2339–2348.
- [17] de Pablo, J. J., Jackson, N. E., Webb, M. A., Chen, L.-Q., Moore, J. E., Morgan, D., Jacobs, R., Pollock, T., Schlom, D. G., Toberer, E. S., et al., "New frontiers for the materials genome initiative," <u>npj Computational Materials</u>, Vol. 5, No. 1, 2019, p. 41.
- [18] Yeratapally, S. R., Glavicic, M. G., Argyrakis, C., and Sangid, M. D., "Bayesian uncertainty quantification and propagation for validation of a microstructure sensitive model for prediction of fatigue crack initiation," <u>Reliability Engineering & System Safety</u>, Vol. 164, 2017, pp. 110–123.

- [19] Venkatraman, A., Mohan, S., Joseph, V. R., McDowell, D. L., and Kalidindi, S. R., "A new framework for the assessment of model probabilities of the different crystal plasticity models for lamellar grains in Titanium alloys," <u>Modelling and Simulation</u> in Materials Science and Engineering, Vol. 31, No. 4, 2023, p. 044001.
- [20] Bandyopadhyay, R., Prithivirajan, V., and Sangid, M. D., "Uncertainty quantification in the mechanical response of crystal plasticity simulations," Jom, Vol. 71, No. 8, 2019, pp. 2612–2624.
- [21] Tran, A., Robbe, P., and Lim, H., "Multi-faceted Uncertainty Quantification for Structure-Property Relationship with Crystal Plasticity Finite Element," TMS Annual Meeting & Exhibition, Springer, 2023, pp. 596–606.
- [22] Acar, P., "Recent progress of uncertainty quantification in small-scale materials science," <u>Progress in Materials Science</u>, Vol. 117, 2021, p. 100723.
- [23] Khadyko, M., Sturdy, J., Dumoulin, S., Hellevik, L. R., and Hopperstad, O. S., "Uncertainty quantification and sensitivity analysis of material parameters in crystal plasticity finite element models," <u>Journal of Mechanics of Materials and Structures</u>, Vol. 13, No. 3, 2018, pp. 379–400.
- [24] Acar, P., "Machine learning reinforced crystal plasticity modeling under experimental uncertainty," <u>AIAA Journal</u>, Vol. 58, No. 8, 2020, pp. 3569–3576.
- [25] "GE Aerospace," http://aiweb.techfak.uni-bielefeld.de/content/bworld-robot-control-software/, 2008. Accessed: 2023-05-10.
- [26] Anand, L., and Kothari, M., "A computational procedure for rate-independent crystal plasticity," <u>Journal of the Mechanics and Physics of Solids</u>, Vol. 44, No. 4, 1996, pp. 525–558.
- [27] Acar, P., Ramazani, A., and Sundararaghavan, V., "Crystal plasticity modeling and experimental validation with an orientation distribution function for ti-7al alloy," Metals, Vol. 7, No. 11, 2017, p. 459.
- [28] Acar, P., "Crystal plasticity model calibration for Ti-7Al alloy with a multi-fidelity computational scheme," <u>Integrating Materials</u> and Manufacturing Innovation, Vol. 7, No. 4, 2018, pp. 186–194.
- [29] Elleithy, M., Zhao, H., and Acar, P., "Sensitivity Assessment on Homogenized Stress-Strain Response of Ti-6Al-4V Alloy," JOM, 2023, pp. 1–10.
- [30] Deka, D., Joseph, D. S., Ghosh, S., and Mills, M. J., "Crystal plasticity modeling of deformation and creep in polycrystalline Ti-6242," <u>Metallurgical and materials transactions A</u>, Vol. 37, 2006, pp. 1371–1388.
- [31] Ghosh, S., and States, J. H. U. B. U., "Multi-Scale Analysis of Deformation and Failure in Polycrystalline Titanium Alloys Under High Strain-Rates," 2015.
- [32] Ozturk, D., Shahba, A., and Ghosh, S., "Crystal plasticity FE study of the effect of thermo-mechanical loading on fatigue crack nucleation in titanium alloys," Fatigue & Fracture of Engineering Materials & Structures, Vol. 39, No. 6, 2016, pp. 752–769.